Nonparaxial propagation of Hermite–Laguerre–Gaussian beams in uniaxial crystal orthogonal to the optical axis*

Xu Yi-Qing (徐一清), Zhou Guo-Quan (周国泉)†, and Wang Xiao-Gang(汪小刚)

School of Sciences, Zhejiang A & F University, Lin'an 311300, *China*

(Received 20 July 2012; revised manuscript received 24 October 2012)

Analytical expressions for the three components of the nonparaxial propagation of a Hermite–Laguerre–Gaussian (HLG) beam in uniaxial crystal orthogonal to the optical axis are derived. The intensity distribution of an HLG beam and its three components propagating in a uniaxial crystal orthogonal to the optical axis are demonstrated by numerical examples. Although the y and z components of an HLG beam in the incident plane are both equal to zero, they emerge upon propagation inside the uniaxial crystal. Moreover, the beam profile of the x component is relatively stable and the beam profiles of the y and z components have the same evolution law. If the ratio of the extraordinary refractive index to the ordinary refractive index is larger than unity, the beam profile of the HLG beam is elongated in the x direction and generally rotates clockwise. Otherwise, the beam profile of the HLG beam is elongated in the y direction and generally rotates anticlockwise. This research is beneficial to the optical trapping and nonlinear optics involved in the rotation of a beam profile.

Keywords: Hermite–Laguerre–Gaussian beam, uniaxial crystal, nonparaxial propagation

PACS: 41.85.Ew, 42.25.Bs, 42.60.Jf, 42.70.–a **DOI:** 10.1088/1674-1056/22/6/064101

1. Introduction

As a structurally stable solution of the parabolic equation, a united family of Hermite–Gaussian (HG) and Laguerre–Gaussian (LG) beams, namely the Hermite–Laguerre–Gaussian (HLG) beam, has been introduced.[1,2] By varying the additional angle parameter in the expression of HLG beams, HLG beams can be transformed from HG beams to LG beams continuously. The HLG beam is structurally stable upon propagation. HLG beams can be experimentally produced by using astigmatic transformation or mode converters.[1,3,4] Based on a recurrence approach, the analytical equations of the propagation of HLG beams through a paraxial optical *ABCD* system with a rectangular hard-edged aperture have been derived.[5] Based on the vectorial Rayleigh–Sommerfeld diffraction integrals, the closed-form expressions of vectorial nonparaxial circularly polarized HLG beams in the far-field have been derived.[6] By means of the extended power in the bucket and the z component of the time-averaged Poynting vector, the far-field properties and beam quality of vectorial nonparaxial HLG beams have been investigated in detail.[7] By using the stationary phase method, the vectorial structure of HLG beams has been demonstrated in the far-field.[8] An exact HLG beam solution of the Snyder–Mitchell mode, which is confirmed by the simulation of the nonlocal nonlinear Schrödinger equation, has been presented.[9] A transformation of an HLG beam in general astigmatic optical systems can be described in terms of rotations in three-dimensional spaces.[10,11] HLG beams can be converted into Gaussian beams by using diffraction gratings.[12] The HLG beam can also be extended to an elegant HLG beam.[13] HLG beams play an important role in resonators and optical waveguides, as well as in optical vortices.[14,15]

Many applications such as the design of the polarizer and the compensator are involved in laser beams propagating in uniaxial crystals. The propagations of various kinds of laser beams in uniaxial crystals have been extensively examined.[16–23] However, no literature in the propagations of HLG beams in uniaxial crystals has been reported. In the remainder of this paper, therefore, the nonparaxial propagation of an HLG beam in uniaxial crystal orthogonal to the optical axis is to be investigated.

2. Nonparaxial propagation equation of an HLG beam in uniaxial crystal orthogonal to the optical axis

In the Cartesian coordinate system, the z axis is taken to be the propagation axis. The optical axis of the uniaxial crystal coincides with the x axis. The input plane is $z = 0$ and the observation plane is z. The dielectric tensor of the uniaxial crystal is described by

$$\varepsilon = \begin{pmatrix} n_{\mathrm{e}}^2 & 0 & 0 \\ 0 & n_{\mathrm{o}}^2 & 0 \\ 0 & 0 & n_{\mathrm{o}}^2 \end{pmatrix}, \tag{1}$$

*Project supported by the National Natural Science Foundation of China (Grant Nos. 10974179 and 61178016), the Natural Science Foundation of Zhejiang Province, China (Grant No. Y1090073), and the Key Project of the Education Commission of Zhejiang Province, China (Grant No. Z201120128).

†Corresponding author. E-mail: zhouguoquan178@sohu.com

© 2013 Chinese Physical Society and IOP Publishing Ltd

where $n_{\rm o}$ and $n_{\rm e}$ are the ordinary and extraordinary refractive indices, respectively. The ratio of the extraordinary refractive index to the ordinary refractive index is defined as $e = n_{\rm e}/n_{\rm o}$. The HLG beam considered here is linearly polarized in the x direction and is incident on a uniaxial crystal in the plane $z = 0$. The HLG beam in the input plane $z = 0$ takes the following form[1,2]

$$\begin{bmatrix} E_x(\rho_0, 0) \\ E_y(\rho_0, 0) \end{bmatrix} = \begin{bmatrix} \phi_{n,m}(x_0, y_0 | \alpha) \\ 0 \end{bmatrix}, \tag{2}$$

with $\phi_{n,m}(x_0, y_0 | \alpha)$ being given by

$$\begin{aligned} &\phi_{n,m}(x_0, y_0 | \alpha) \\ &= \exp\left(-\frac{x_0^2 + y_0^2}{2w_0^2}\right) \sum_{j=0}^{n+m} \mathrm{i}^j (\cos\alpha)^{n-j} (\sin\alpha)^{m-j} \\ &\quad \times \mathrm{P}_j^{(n-j,m-j)}(-\cos 2\alpha) H_{n+m-j}\left(\frac{x_0}{w_0}\right) H_j\left(\frac{y_0}{w_0}\right), \end{aligned} \tag{3}$$

where

$$\begin{aligned} &\mathrm{P}_j^{(n-j,m-j)}(-\cos 2\alpha) \\ &= 2^{-j} \sum_{l=0}^{j} \binom{n}{l} \binom{m}{j-l} (-1-\cos 2\alpha)^{j-l} (1-\cos 2\alpha)^l \end{aligned} \tag{4}$$

is the Jacobi polynomial, $\boldsymbol{\rho}_0 = x_0 \boldsymbol{e}_x + y_0 \boldsymbol{e}_y$, $\boldsymbol{e}_x$ and $\boldsymbol{e}_y$ are the unit vectors in the x and y directions, respectively, $H_j(\cdot)$ is the j-th order Hermite polynomial, n and m are the transverse mode numbers in the x and y directions, respectively, w_0 is the Gaussian waist width, and α is an angle parameter which allows to make a continuous transition from HG to LG beam. When α is equal to 0, the HLG beam reduces to an HG beam. When α is equal to $\pi/4$, the HLG beam transforms to an LG beam.

The propagation of the HLG beam in uniaxial crystal orthogonal to the optical axis obeys the following equation:[24]

$$\begin{aligned} \boldsymbol{E}(\boldsymbol{\rho}, z) &= \iint_{-\infty}^{\infty} \mathrm{d}^2\boldsymbol{k} \exp(\mathrm{i}\boldsymbol{k}\cdot\boldsymbol{\rho}) \\ &\quad \times \exp(\mathrm{i}k_{\rm ez} z) \begin{pmatrix} \tilde{E}_x(\boldsymbol{k}) \\ -\dfrac{k_x k_y}{k_0^2 n_{\rm o}^2 - k_x^2} \tilde{E}_x(\boldsymbol{k}) \\ -\dfrac{k_{\rm ez} k_x}{k_0^2 n_{\rm o}^2 - k_x^2} \tilde{E}_x(\boldsymbol{k}) \end{pmatrix} \\ &\quad + \iint_{-\infty}^{\infty} \mathrm{d}^2\boldsymbol{k} \exp(\mathrm{i}\boldsymbol{k}\cdot\boldsymbol{\rho}) \\ &\quad \times \exp(\mathrm{i}k_{\rm ez} z) \begin{pmatrix} 0 \\ -\dfrac{k_x k_y}{k_0^2 n_{\rm o}^2 - k_x^2} \tilde{E}_x(\boldsymbol{k}) + \tilde{E}_y(\boldsymbol{k}) \\ -\dfrac{k_y}{k_{\rm oz}} \left[\dfrac{k_x k_y}{k_0^2 n_{\rm o}^2 - k_x^2} \tilde{E}_x(\boldsymbol{k}) \tilde{E}_y(\boldsymbol{k})\right] \end{pmatrix}, \end{aligned} \tag{5}$$

where $\boldsymbol{k} = k_x \boldsymbol{e}_x + k_y \boldsymbol{e}_y$, $\boldsymbol{\rho} = x\boldsymbol{e}_x + y\boldsymbol{e}_y$, and $k_0 = 2\pi/\lambda$ is the wave number with λ being the optical wavelength; $\tilde{E}_s(\boldsymbol{k})$ is the two-dimensional Fourier transform of the transverse components of the optical field in the plane $z = 0$ and is given by

$$\begin{aligned} \tilde{\boldsymbol{E}}_{\rm s}(\boldsymbol{k}) &= \frac{1}{(2\pi)^2} \iint_{-\infty}^{\infty} E_{\rm s}(\boldsymbol{\rho}_0, 0) \\ &\quad \times \exp[\mathrm{i}(k_x x_0 + k_y y_0)] \mathrm{d}x_0 \mathrm{d}y_0, \end{aligned} \tag{6}$$

where $s = x$ or y (hereafter). $k_{\rm ez}$ and $k_{\rm oz}$ are defined by

$$k_{\rm ez} = [k_0^2 n_{\rm e}^2 - e^2 k_x^2 - k_y^2]^{1/2}, \quad k_{\rm oz} = (k_{\rm o}^2 n_0^2 - k_x^2 - k_y^2)^{1/2}. \tag{7}$$

To describe the nonparaxial propagation of the HLG beam in a uniaxial crystal, Eq. (5) can be approximately expressed as a sum of the paraxial field and a nonparaxial correction term[24]

$$\begin{aligned} \boldsymbol{E}(\boldsymbol{\rho}, z) &= \exp(\mathrm{i}k_0 n_{\rm e} z) \iint_{-\infty}^{\infty} \mathrm{d}^2\boldsymbol{k} \exp(\mathrm{i}\boldsymbol{k}\cdot\boldsymbol{\rho}) \\ &\quad \times \exp\left(-\mathrm{i}\frac{e^2 k_x^2 + k_y^2}{2k_0 n_{\rm e}} z\right) \begin{pmatrix} \tilde{E}_x(\boldsymbol{k}) \\ -\dfrac{k_x k_y}{k_0^2 n_{\rm o}^2} \tilde{E}_x(\boldsymbol{k}) \\ -\dfrac{e k_x}{k_0 n_{\rm o}} \tilde{E}_x(\boldsymbol{k}) \end{pmatrix} \\ &\quad + \exp(\mathrm{i}k_0 n_{\rm o} z) \iint_{-\infty}^{\infty} \mathrm{d}^2\boldsymbol{k} \exp(\mathrm{i}\boldsymbol{k}\cdot\boldsymbol{\rho}) \\ &\quad \times \exp\left(-\mathrm{i}\frac{k_x^2 + k_y^2}{2k_0 n_{\rm o}} z\right) \begin{pmatrix} 0 \\ \dfrac{k_x k_y}{k_0^2 n_{\rm o}^2} \tilde{E}_x(\boldsymbol{k}) + \tilde{E}_y(\boldsymbol{k}) \\ -\dfrac{k_y}{k_{\rm o} n_{\rm o}} \tilde{E}_y(\boldsymbol{k}) \end{pmatrix}. \end{aligned} \tag{8}$$

By using the property of the Fourier transform,[25] the three components of the nonparaxial field of an HLG beam in the uniaxial crystal orthogonal to the optical axis can also be rewritten as

$$E_x(\boldsymbol{\rho}, z) = \frac{n_{\rm o}}{\mathrm{i}\lambda z} \iint_{-\infty}^{\infty} E_x(\boldsymbol{\rho}_0, 0) \Pi_{\rm e}(\boldsymbol{\rho}, \boldsymbol{\rho}_0) \mathrm{d}x_0 \mathrm{d}y_0, \tag{9}$$

$$\begin{aligned} E_y(\boldsymbol{\rho}, z) &= \frac{\mathrm{i}n_{\rm o}}{\lambda z^3} \iint_{-\infty}^{\infty} (x - x_0)(y - y_0) E_x(\boldsymbol{\rho}_0, 0) \\ &\quad \times [\Pi_{\rm e}(\boldsymbol{\rho}, \boldsymbol{\rho}_0) - \Pi_{\rm o}(\boldsymbol{\rho}, \boldsymbol{\rho}_0)] \mathrm{d}x_0 \mathrm{d}y_0 \\ &\quad + \frac{n_{\rm o}}{\mathrm{i}\lambda z} \iint_{-\infty}^{\infty} E_y(\boldsymbol{\rho}_0, 0) \Pi_{\rm o}(\boldsymbol{\rho}, \boldsymbol{\rho}_0) \mathrm{d}x_0 \mathrm{d}y_0, \end{aligned} \tag{10}$$

$$\begin{aligned} E_z(\boldsymbol{\rho}, z) &= \frac{\mathrm{i}n_{\rm o}}{\lambda z^2} \iint_{-\infty}^{\infty} [(x - x_0) E_x(\boldsymbol{\rho}_0, 0) \Pi_{\rm e}(\boldsymbol{\rho}, \boldsymbol{\rho}_0) \\ &\quad + (y - y_0) E_y(\boldsymbol{\rho}_0, 0) \Pi_{\rm o}(\boldsymbol{\rho}, \boldsymbol{\rho}_0)] \mathrm{d}x_0 \mathrm{d}y_0, \end{aligned} \tag{11}$$

with $\Pi_{\rm e}(\boldsymbol{\rho}, \boldsymbol{\rho}_0)$ and $\Pi_{\rm o}(\boldsymbol{\rho}, \boldsymbol{\rho}_0)$ being given by

$$\begin{aligned} &\Pi_{\rm e}(\boldsymbol{\rho}, \boldsymbol{\rho}_0) \\ &= \exp(\mathrm{i}ek_0 n_{\rm o} z) \exp\left\{-\frac{k_0 n_{\rm o}}{2\mathrm{i}ez} \left[(x - x_0)^2 + e^2 (y - y_0)^2\right]\right\}, \end{aligned} \tag{12}$$

$$\begin{aligned} &\Pi_{\rm o}(\boldsymbol{\rho}, \boldsymbol{\rho}_0) \\ &= \exp(\mathrm{i}k_0 n_{\rm o} z) \exp\left\{-\frac{k_0 n_{\rm o}}{2\mathrm{i}z} \left[(x - x_0)^2 + (y - y_0)^2\right]\right\}. \end{aligned} \tag{13}$$

By using the following mathematical formulae[25]

$$\int_{-\infty}^{\infty} H_j(x)\exp[-(x-y)^2/\delta]\,\mathrm{d}x = \sqrt{\pi\delta}(1-\delta)^{j/2}H_j[y(1-\delta)^{-1/2}], \tag{14}$$

$$xH_j(x) = 0.5H_{j+1}(x) + jH_{j-1}(x), \tag{15}$$

the three components of the HLG beam in the uniaxial crystal orthogonal to the optical axis are found to be

$$\begin{aligned} &E_x(\rho,z) \\ &= \frac{n_\mathrm{o}}{\mathrm{i}\lambda z}\exp(\mathrm{i}ek_0n_\mathrm{o}z)\sum_{j=0}^{n+m}\mathrm{i}^j(\cos\alpha)^{n-j}(\sin\alpha)^{m-j} \\ &\times P_j^{(n-j,m-j)}(-\cos 2\alpha)\Omega_{n+m-j}(x)U_j(y), \end{aligned} \tag{16}$$

$$\begin{aligned} &E_y(\rho,z) \\ &= \frac{\mathrm{i}n_\mathrm{o}}{\lambda z^3}\Bigg\{\exp(\mathrm{i}ek_0n_\mathrm{o}z)\sum_{j=0}^{n+m}\mathrm{i}^j(\cos\alpha)^{n-j}(\sin\alpha)^{m-j} \\ &\times P_j^{(n-j,m-j)}(-\cos 2\alpha)\{xy\Omega_{n+m-j}(x)U_j(y) - w_0x \\ &\times \Omega_{n+m-j}(x) \\ &\times [0.5U_{j+1}(y) + jU_{j-1}(y)] - w_0y[0.5\Omega_{n+m+1-j}(x) \\ &+ (n+m-j)\Omega_{n+m-j-1}(x)]U_j(y) \\ &+ w_0^2[0.5\Omega_{n+m+1-j}(x) + (n+m-j)\Omega_{n+m-j-1}(x)] \\ &\times [0.5U_{j+1}(y) + jU_{j-1}(y)]\} - \exp(\mathrm{i}k_0n_\mathrm{o}z) \\ &\times \sum_{j=0}^{n+m}\mathrm{i}^j(\cos\alpha)^{n-j}(\sin\alpha)^{m-j}P_j^{(n-j,m-j)}(-\cos 2\alpha) \\ &\times \{xyV_{n+m-j}(x)V_j(y) - w_0xV_{n+m-j}(x) \\ &\times [0.5V_{j+1}(y) + jV_{j-1}(y)] - w_0y[0.5V_{n+m+1-j}(x) \\ &+ (n+m-j)V_{n+m-j-1}(x)]V_j(y) + w_0^2 \\ &\times [0.5V_{n+m+1-j}(x) + (n+m-j)V_{n+m-j-1}(x)] \\ &\times [0.5V_{j+1}(y) + jV_{j-1}(y)]\}\Bigg\}, \end{aligned} \tag{17}$$

$$\begin{aligned} &E_z(\rho,z) \\ &= \frac{\mathrm{i}n_\mathrm{o}}{\lambda z^2}\exp(\mathrm{i}ek_0n_\mathrm{o}z)\sum_{j=0}^{n+m}\mathrm{i}^j(\cos\alpha)^{n-j}(\sin\alpha)^{m-j} \\ &\times P_j^{(n-j,m-j)}(-\cos 2\alpha)\{x\Omega_{n+m-j}(x)U_j(y) \\ &- w_0[0.5\Omega_{n+m+1-j}(x) + (n+m-j) \\ &\times \Omega_{n+m-j-1}(x)]U_j(y)\}, \end{aligned} \tag{18}$$

with $\Omega_\mu(x)$, $U_\mu(x)$, $V_\mu(x)$, and $V_\mu(y)$ being given by

$$\begin{aligned} \Omega_\mu(x) &= w_0\sqrt{\pi\delta}(1-\delta)^{\mu/2} \\ &\times \exp(-ax^2)H_\mu\left[\frac{\delta z_\mathrm{r}n_\mathrm{o}}{\mathrm{i}ezw_0(1-\delta)^{1/2}}\right], \end{aligned} \tag{19}$$

$$\begin{aligned} U_\mu(y) &= w_0\sqrt{\pi\beta}(1-\beta)^{\mu/2} \\ &\times \exp(-by^2)H_\mu\left[\frac{\beta z_\mathrm{r}en_\mathrm{o}y}{\mathrm{i}zw_0(1-\beta)^{1/2}}\right], \end{aligned} \tag{20}$$

$$\begin{aligned} V_\mu(s) &= w_0\sqrt{\pi\gamma}(1-\gamma)^{\mu/2} \\ &\times \exp(-cs^2)H_\mu\left[\frac{\gamma z_\mathrm{r}n_0s}{\mathrm{i}zw_0(1-\gamma)^{1/2}}\right], \end{aligned} \tag{21}$$

where μ is an arbitrary integer. The auxiliary parameters are defined as

$$\delta = \left(\frac{1}{2} - \frac{\mathrm{i}z_\mathrm{r}n_\mathrm{o}}{ez}\right)^{-1}, \tag{22}$$

$$\beta = \left(\frac{1}{2} - \frac{\mathrm{i}ez_\mathrm{r}n_\mathrm{o}}{z}\right)^{-1}, \tag{23}$$

$$\gamma = \left(\frac{1}{2} - \frac{\mathrm{i}z_\mathrm{r}n_0}{z}\right)^{-1}, \tag{24}$$

$$a = -\delta\left(\frac{z_\mathrm{r}n_\mathrm{o}}{\mathrm{i}ezw_0}\right)^2 + \frac{k_0n_\mathrm{o}}{2iez}, \tag{25}$$

$$b = -\beta\left(\frac{ez_\mathrm{r}n_\mathrm{o}}{\mathrm{i}zw_0}\right)^2 + \frac{ek_0n_\mathrm{o}}{2\mathrm{i}z}, \tag{26}$$

$$c = -\gamma\left(\frac{z_\mathrm{r}n_\mathrm{o}}{\mathrm{i}zw_0}\right)^2 + \frac{k_0n_\mathrm{o}}{2\mathrm{i}z}, \tag{27}$$

where $z_\mathrm{r} = k_0w_0^2/2$ is the Rayleigh length of the Gaussian part. The y component of the nonparaxial correction is of the second order in the paraxiality regime, whereas the z component is of the first order, which entails that the z component in the slightly nonparaxial regime is stronger than the y component.[24] The paraxial propagation of an HLG beam in the uniaxial crystal orthogonal to the optical axis is included in the above result. Under the paraxial approximation, the propagation of an HLG beam in the uniaxial crystal orthogonal to the optical axis is just given by Eq. (15), and the other two components are equal to zero.

3. Numerical results and analyses

Now we illustrate the propagation properties of an HLG beam in the uniaxial crystal orthogonal to the optical axis. The calculation parameters are chosen as follows: $n = 2$, $m = 1$, $w_0 = \lambda$, $n_\mathrm{o} = 2.616$, and $e = 1.5$. Figures 1–3 show the contours of the intensity distribution of the three components of an HLG beam propagating in the uniaxial crystal orthogonal to the optical axis in several observation planes. Figures 1–3 correspond to $z = 0.1z_\mathrm{r}$, $z = 3z_\mathrm{r}$, and $z = 6z_\mathrm{r}$, respectively. The intensity is proportional to the scale of $1/\lambda^2$, which is omitted in the label of the intensity in each of the figures (where a.u. stands for arbitrary units). In the panels of one figure, the scale of the coordinates and the label of the intensity are the same and may not be marked to make the figure compact. From the top to the bottom of the figure, the angle parameter α is varied from 0 to $\pi/4$ in steps of $\pi/16$. The left, the middle, and the right columns correspond to $|E_x(\rho,z)|^2$, $|E_y(\rho,z)|^2$, and $|E_z(\rho,z)|^2$, respectively. Though the y and z components of an HLG beam in the input plane are zero, they are no longer equal to zero upon propagation in the uniaxial crystal, which can be

interpreted as follows. The y and z components are affected by the x component because of the dependence on $\tilde{E}_x(\boldsymbol{k})$, and this corresponds to a change of polarization state of the radiation that occurs during propagation in the uniaxial crystal.[24] The magnitude of the intensity of the z component is smaller than that of the x component. However, the magnitude of the intensity of the y component is far smaller than those of x and z components. The beam profiles of the three components vary with angle parameter α. From the top to the bottom of the figure, however, one can find the process of evolvement from HG beams to LG beams.

Upon propagation in the uniaxial crystal orthogonal to the optical axis, the spreading of the beam profile in the y direction is far slower than that in the x direction, which is caused by the anisotropic effect of the crystal. When $\alpha \neq 0$, the beam profile of the x component rotates clockwise upon propagation in the uniaxial crystal. Upon propagation in the uniaxial crystal orthogonal to the optical axis, the beam profile of the x component is relatively stable except the rotation. Upon propagation in the uniaxial crystal, however, the beam profiles of the y and z components will evolve and have the same evolution law. Upon propagation in the uniaxial crystal orthogonal to the optical axis, the subordinate lobes in the beam profiles of the y and z components will evolve into predominant lobes. On the contrary, the predominant lobes in the beam profiles of the y and z components will evolve into subordinate lobes.

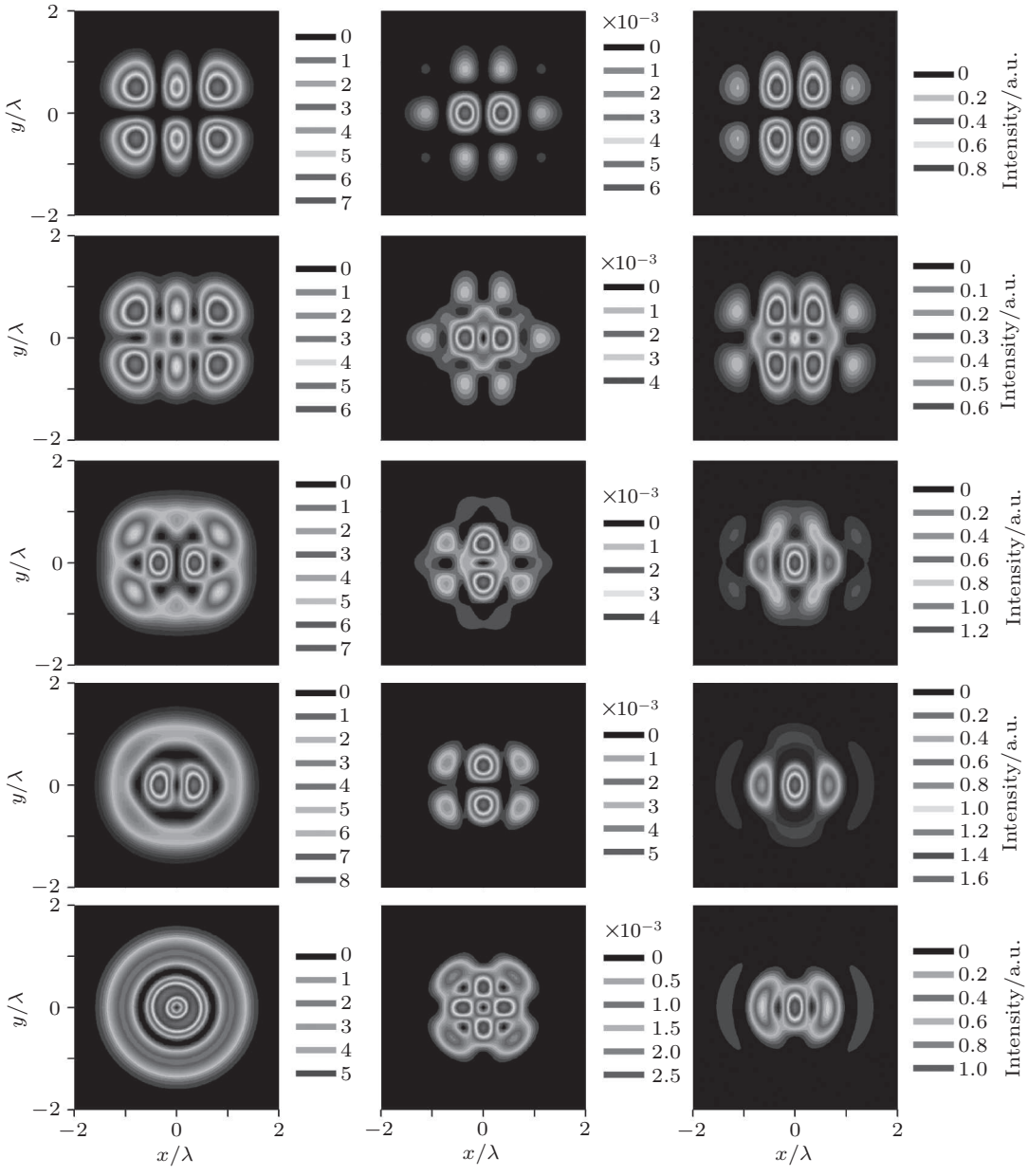


Fig. 1. Contours of the intensity of the three components of an HLG beam in the observation plane $z = 0.1z_r$ of the uniaxial crystal.

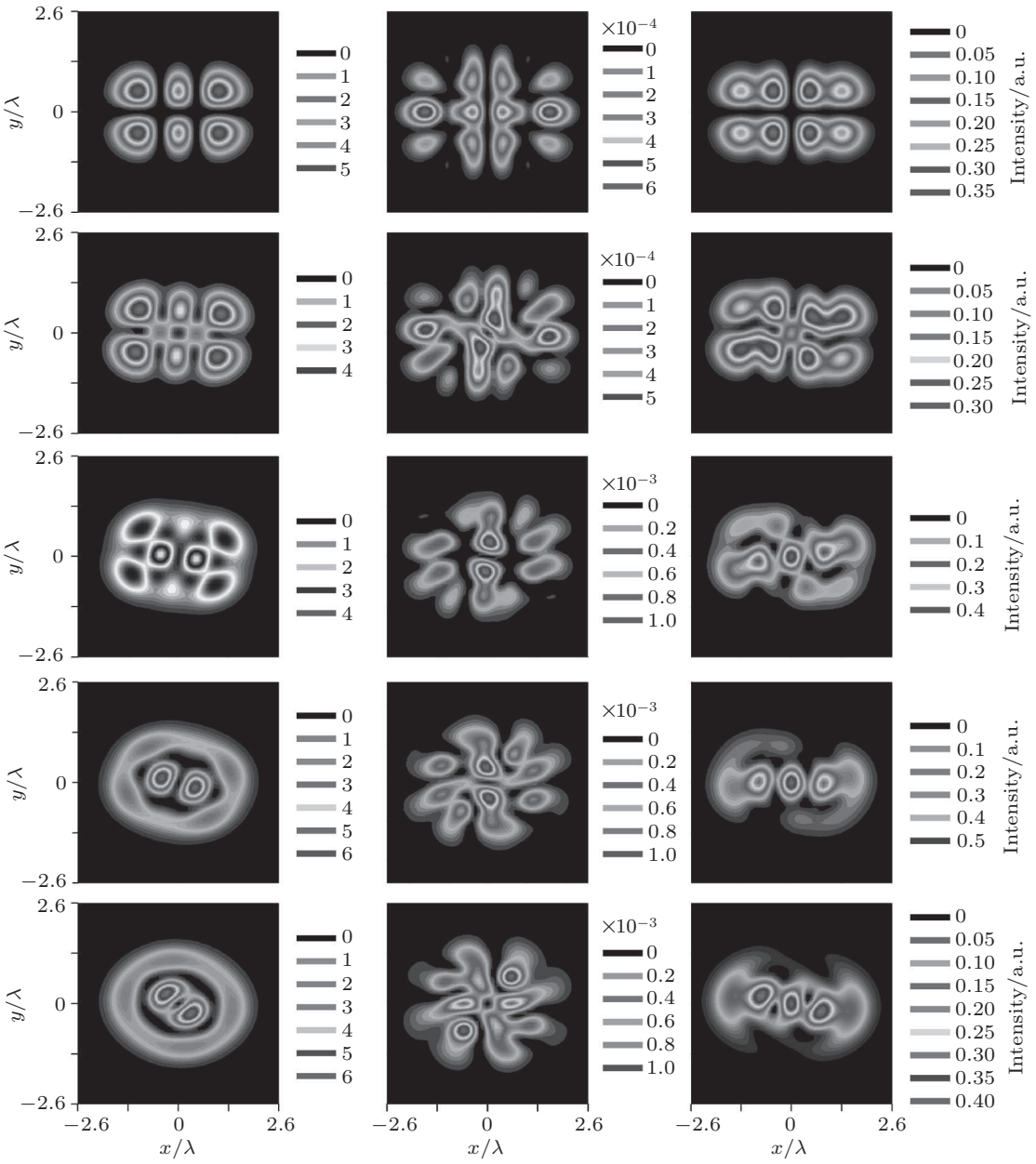


Fig. 2. Contours of the intensity of the three components of an HLG beam in the observation plane $z = 3z_r$ of the uniaxial crystal.

Figure 4 shows the effect of the uniaxial crystal on the beam profile of the HLG beam. In Fig. 4, $\alpha = 3\pi/16$, $z = 3z_r$, and other beam parameters are kept unchanged. When $e > 1$, the beam profile of the HLG beam is elongated in the x direction, and the rotation of the beam profile of the HLG beam is clockwise upon propagation in the uniaxial crystal. If $e < 1$, the beam profile of the HLG beam is elongated in the y direction, and the rotation of the beam profile of the HLG beam is anticlockwise upon propagation in the uniaxial crystal. The contours of the intensity distribution of an HLG beam propagating in the uniaxial crystal orthogonal to the optical axis at several observation planes are shown in Fig. 5. The left, the middle, and the right columns correspond to $z = 0.1z_r$, $z = 3z_r$, and $z = 6z_r$, respectively. The beam profile of an HLG beam is close to that of the x component. The magnitude of the intensity of the HLG beam is larger than that of its x component, which is not distinguished between the corresponding figures as the label of the intensity is marked in the rank. Moreover, the details of the beam profile between the HLG beam and its x component are different. When propagating from the input plane, the central ring in the beam profile of the HLG beam with $\alpha = \pi/4$ will split into two lobes. Moreover, the distance between the two lobes increases with propagation distance increasing.

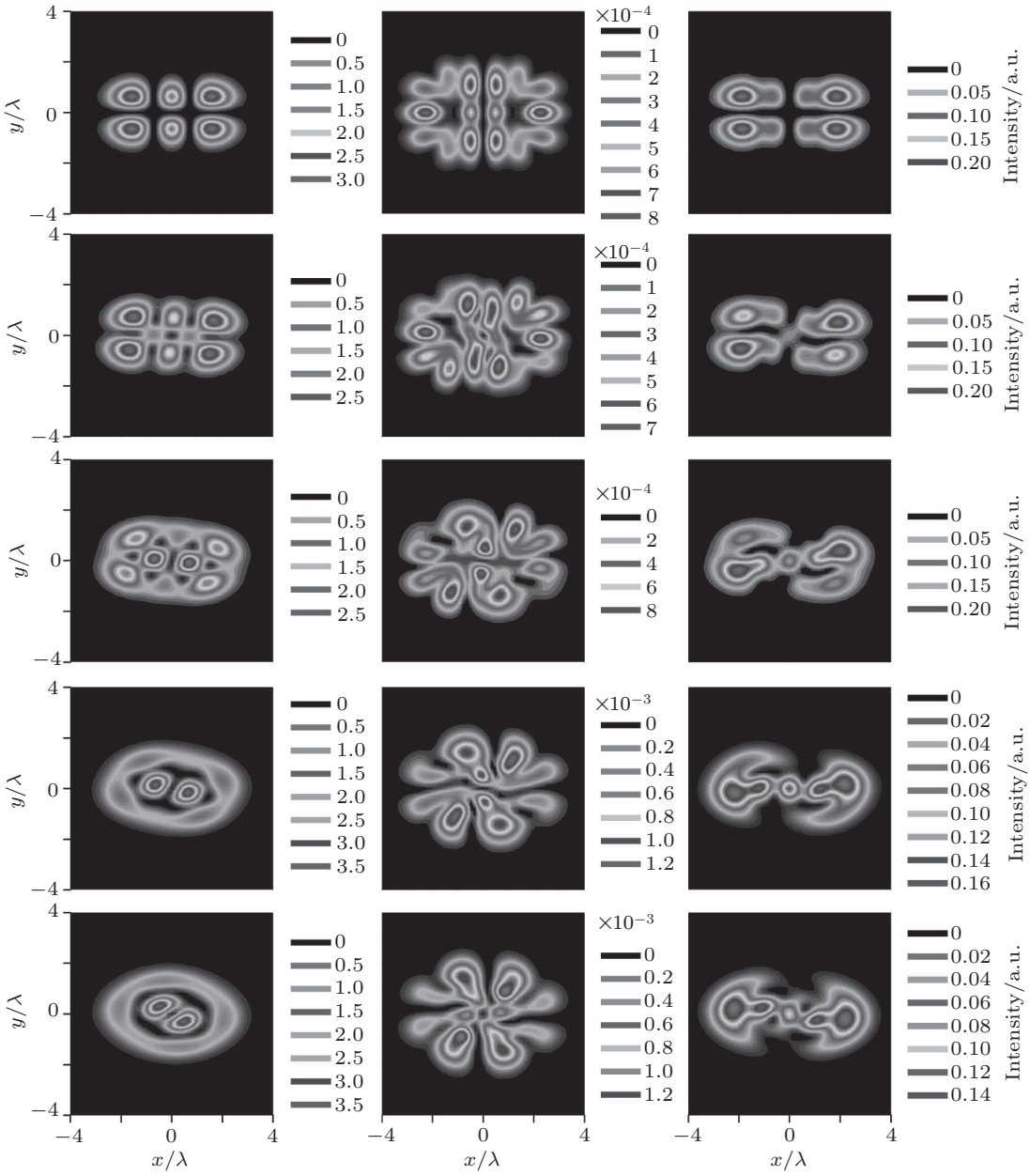


Fig. 3. Contours of the intensity of the three components of an HLG beam in the observation plane $z = 6z_r$ of the uniaxial crystal.

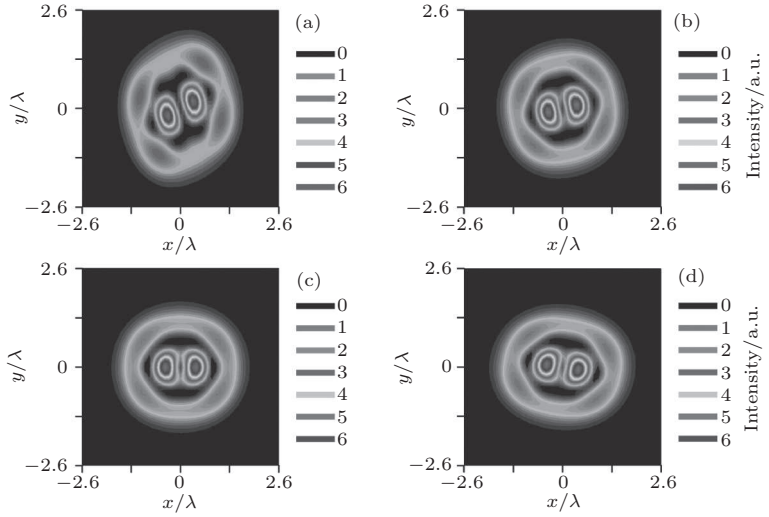


Fig. 4. Contours of the intensity of an HLG beam in the observation plane $z = 3z_r$ of different uniaxial crystals, for the cases of $e = 0.6$ (a), 0.8 (b), 1.0 (c), and 1.2 (d).

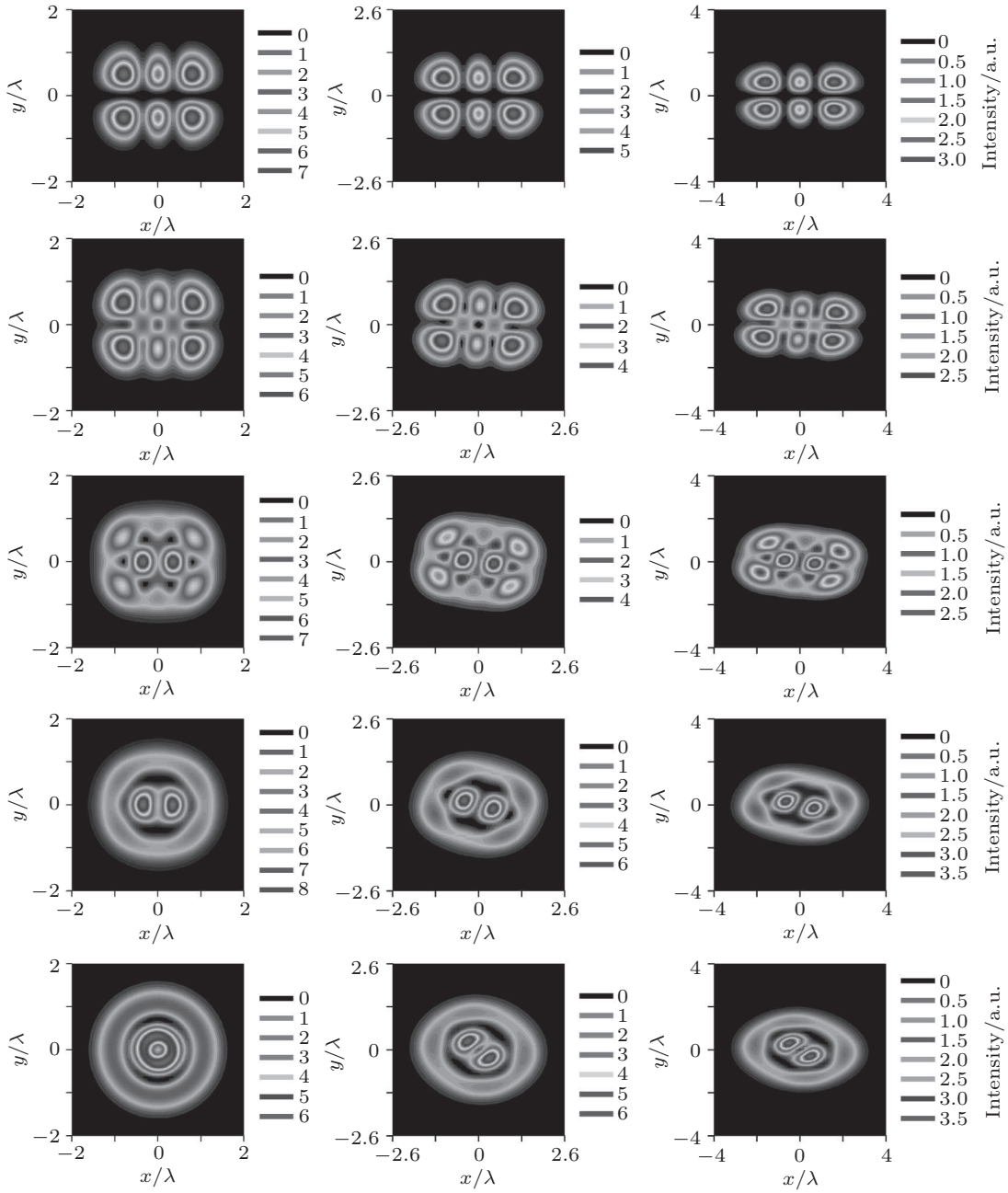


Fig. 5. Contours of the intensity of an HLG beam in several observation planes of the uniaxial crystal.

4. Conclusions

The analytical nonparaxial formula of an HLG beam propagating in a uniaxial crystal orthogonal to the optical axis is derived. The intensity distributions of the HLG beam and its three components propagating in a uniaxial crystal orthogonal to the optical axis are demonstrated by numerical examples. Though the y and z components of an HLG beam in the input plane are both zero, the y and z components emerge upon propagation in the uniaxial crystal. The magnitude of the intensity of the z component is smaller than that of the x component, and the magnitude of the intensity of the y component is far smaller than those of x and z components. The beam profiles of the three components vary with angle parameter α. Upon propagation in the uniaxial crystal, the beam profile of the x component is relatively stable and the beam profiles of the y and z components have the same evolution law. When the Gaussian waist width is comparable to the wavelength, the y and z components cannot be ignored. When propagating in the uniaxial crystal with $e > 1$, the beam profile of the HLG beam is elongated in the x direction, and the rotation of the beam profile of the HLG beam with $\alpha \neq 0$ is clockwise. When propagating in the uniaxial crystal with $e < 1$, the beam profile of the HLG beam is elongated in the y direction, and the rotation of the beam profile of the HLG beam with $\alpha \neq 0$ is anticlock-

wise. The beam profile of the HLG beam can be modulated by the uniaxial crystal. This research is beneficial to the optical trapping and nonlinear optics involved in the rotation of the beam profile.

References

[1] Abramochkin E G and Volostnikov V G 2004 *J. Opt. A: Pure Appl. Opt.* **6** S157
[2] Abramochkin E G and Volostnikov V G 2010 *Phys. Wave Phenom.* **18** 14
[3] Courtial J and Padgett M J 1999 *Opt. Commun.* **159** 13
[4] Malyutin A A 2004 *Quantum Electron.* **34** 165
[5] Duan K L and Lü B D 2005 *Opt. Commun.* **250** 1
[6] He Z, Kang X P and Lü B D 2006 *Acta Phys. Sin.* **55** 4574 (in Chinese)
[7] Kang X P, He Z and Lü B D 2007 *Opt. Laser Technol.* **39** 1046
[8] Zhou G Q and Zheng J 2008 *Opt. Laser Technol.* **40** 858
[9] Deng D M, Guo Q and Hu W 2008 *J. Phys. B: At. Mol. Opt. Phys.* **41** 225402
[10] Abramochkin E G, Razueva E V and Volostnikov V G 2008 *Proc. SPIE* **7009** 70090
[11] Abramochkin E G, Razueva E V and Volostnikov V G 2010 *J. Opt. Soc. Am. A* **27** 2506
[12] Syouji A, Kurihara K, Otomo A and Saito S 2010 *Appl. Opt.* **49** 1513
[13] Deng D M and Guo Q 2008 *Opt. Lett.* **33** 1225
[14] Flossmann F, Schwarz U T and Maier M 2005 *Opt. Commun.* **250** 218
[15] Volpe G and Petrov D 2004 *Opt. Commun.* **237** 89
[16] Ciattoni A, Cincotti G and Palma C 2002 *J. Opt. Soc. Am. A* **19** 792
[17] Cincotti G, Ciattoni A and Palma C 2002 *J. Opt. Soc. Am. A* **19** 1680
[18] Lü B D and Luo S R 2004 *Opt. Laser Technol.* **36** 51
[19] Liu D J and Zhou Z X 2008 *J. Opt. A: Pure Appl. Opt.* **10** 095005
[20] Deng D G, Yu H, Xu S Q, Shao J D and Fan Z X 2008 *Opt. Commun.* **281** 202
[21] Tang B 2009 *J. Opt. Soc. Am. A* **26** 2480
[22] Zhao C L and Cai Y J 2010 *J. Mod. Opt.* **57** 375
[23] Zhou G Q 2012 *Chin. Phys. B* **21** 054104
[24] Ciattoni A and Palma C 2003 *J. Opt. Soc. Am. A* **20** 2163
[25] Gradshteyn I and Ryzhik I 1980 *Table of Integrals, Series, and Products* (New York: Academic Press)